

A study of free-volume hole distributions in $x\text{TiO}_2 \cdot (1 - x)\text{SiO}_2$ by positron annihilation spectroscopy

This article has been downloaded from IOPscience. Please scroll down to see the full text article.

1996 J. Phys.: Condens. Matter 8 6313

(<http://iopscience.iop.org/0953-8984/8/34/018>)

View [the table of contents for this issue](#), or go to the [journal homepage](#) for more

Download details:

IP Address: 171.66.16.206

The article was downloaded on 13/05/2010 at 18:34

Please note that [terms and conditions apply](#).

A study of free-volume hole distributions in $x\text{TiO}_2 \cdot (1-x)\text{SiO}_2$ by positron annihilation spectroscopy

M A Misheva†, N Djourelov†, F M A Margaca‡, I M Miranda Salgado§
and G Passage||

† Faculty of Physics, Sofia University, 1126 Sofia, Bulgaria

‡ Physics Department, ITN, 2685 Sacavem, Portugal

§ Glass and Ceramics Engineering Department, University of Aveiro, 3800 Aveiro, Portugal

|| Institute of Nuclear Research and Nuclear Energy, 1784 Sofia, Bulgaria

Received 22 January 1996

Abstract. Positron annihilation spectroscopy has been used to obtain information about the small-pore structure of the system $x\text{TiO}_2 \cdot (1-x)\text{SiO}_2$ ($x = 10, 30$ mol%). The pore radius probability distribution functions have been obtained from the ortho-positronium lifetime probability distribution functions, determined from lifetime spectra using the CONTIN (PALS-2) program. The linearity of the variation of S versus W has been used to check the similarity of (or difference between) the defect structures of the samples prepared under different experimental conditions.

1. Introduction

Glasses of the system $\text{TiO}_2\text{--SiO}_2$ have a high refractoriness and low thermal expansion coefficient. Their preparation is very difficult using the traditional oxide melting method because of the high melting point of TiO_2 . Furthermore, devitrification cannot be avoided for αTiO_2 content larger than $\simeq 12\%$ [1].

Materials of system $x\text{TiO}_2 \cdot (1-x)\text{SiO}_2$ can be prepared by a sol–gel, e.g. alkoxide, method for any value of x at relatively low temperature [2]. However, the final product is porous and densification occurs on heat treatment.

Small-angle neutron scattering (SANS) studies [3] showed that $x\text{TiO}_2 \cdot (1-x)\text{SiO}_2$ xerogels heat treated at 120°C with $x = 2, 4$ and 6 mol% consist of homogeneous regions of about 12 nm average diameter and pores of about 3.6 nm average diameter located in the free space left by the contact of those regions. Samples heat treated at 120°C contain a large concentration of chemisorbed hydroxyls on the surface of the pores, since desorption of these hydroxyls only occurs at about 550°C . The 850°C heat-treated xerogels showed a similar microstructure with slightly decreased size for both oxide regions and pores. For this material x-ray diffraction showed [3] a small amount of crystalline TiO_2 (anatase) in a solid solution of amorphous SiO_2 .

The often-used methods for investigation of the pores—photochromic and fluorescence spectroscopy when the free-volume holes in a material are only of a few ångströms in size ($2\text{--}20$ Å)—are not suitable because of the significant perturbation that they introduce by incorporating a sizeable probe into the holes. Small-angle neutron and x-ray scattering cannot effectively reveal the properties of holes whose size is less than 20 Å either [4].

Recently positron annihilation lifetime (PAL) spectroscopy has been successfully used for studying the free-volume holes in porous materials such as protective coatings [5], silica gels [6] and polymers [7, 8, 9]. The method is based on the established fact that the ortho-positronium 'atom' (o-Ps), a bound state of the positron and the electron, is preferentially localized in the free-volume holes, where the o-Ps lifetime is dependent on the hole size [6, 10]. It is considered that o-Ps formation probability is proportional to the concentration of holes.

In this paper we present results on the positron annihilation in the system $x\text{TiO}_2 \cdot (1 - x)\text{SiO}_2$ ($x = 10, 30$ mol%), obtained by means of the lifetime technique and Doppler broadening of the annihilation 511 keV γ -line.

2. Experimental details

2.1. Samples

The $x\text{TiO}_2 \cdot (1 - x)\text{SiO}_2$ xerogels with $x = 10$ and 30 mol% were prepared using tetraethylorthosilicate (TEOS) and titanium isopropoxide (i-PrTi) as raw materials [2]. TEOS was first hydrolysed for two hours with magnetic stirring at room temperature with water, ethanol and HCl. After this first step, i-PrTi dissolved in ethanol was added to the hydrolysed TEOS solution. Next, water was added until the final $\text{H}_2\text{O}/\text{alkoxides}$ molar ratio, R_{wa} , was attained.

The solutions obtained were left in a glass container covered with a plastic foil at 60 °C for gelation. After a period of 15 days the gels were heat treated at 120 °C for 48 hours, after which one pair of the samples was heat treated for 5.5 hours at 850 °C. The rate of heating to 850 °C was equal to 60 °C h^{-1} .

The experimental conditions for the samples are shown in table 1. The samples were produced in such a way that the influence of some of the processing parameters could be obtained.

Table 1. Experimental conditions for the samples.

No	TiO ₂ (mol%)	R_{wa}	R_{ea}	Heat treatment
1	10	4	10.0	120 °C
2	10	4	2.8	120 °C
3	10	40	2.8	120 °C
4	10	40	2.8	850 °C
5	30	40	10.0	120 °C

Samples 1 and 5 were prepared with an ethanol/alkoxides molar ratio R_{ea} , which was about three times that used for all of the other samples. The influence of this ratio can be studied by comparison of samples 1 and 2. To check the influence of heat treatment, samples 3 and 4 have been studied. Samples 2 and 3 have different H_2O contents. Sample 5 has a large TiO_2 content.

The differential thermal analysis showed [3] that for water content $R_{wa} \leq 10$ at 120 °C there are still some non-hydrolysed organic groups present in the samples: Ti-OR and Si-OR, whose combustion occurs at 250–450 °C. However, for $R_{wa} = 40$ and all x , hydrolysis is complete.

2.2. Positron annihilation lifetimes

The lifetime spectrometer was a standard fast-fast coincidence apparatus based on Pilot U scintillators, XP 2020-Q PMT and ORTEC electronics. It provides a time resolution ~ 260 ps FWHM. The channel width of the multi-channel analyser was $\Delta = 36$ ps/channel. The positron source prepared by $^{22}NaCl$ solution evaporated on and covered by 1 mg cm^{-2} Kapton foils was sandwiched between two identical glass samples. The activity of the source was $12 \pm 1 \text{ } \mu\text{Ci}$. Approximately 3×10^5 counts could be collected for one hour. As a rule, four lifetime spectra were recorded for each pair of samples.

2.3. Data analysis of PAL spectra

2.3.1. Analysis with the POSITRONFIT EXTENDED program [11]. In this case it is considered that positrons annihilate in several strictly defined states, and a finite-term model spectrum is assumed. The lifetime spectrum, $N(t)$, obtained from a positron annihilation experiment is represented by the convolution of the instrumental resolution function, $I(t)$, and the decay curve of positrons, $C(t)$:

$$N(t) = N_s I(t) * C(t) \quad (1)$$

$$C(t) = \sum_{i=1}^n \alpha_i \lambda_i \exp(-\lambda_i t) \quad (2)$$

where n is the number of annihilation modes, α_i is the fraction of positrons annihilating with lifetime $\tau_i = 1/\lambda_i$, and N_s is the total number of the annihilation events.

The instrumental resolution function in our analysis was represented by one gaussian with ~ 260 ps FWHM. As we were interested in the longer-lifetime components, we summarized the content of the adjacent channels two by two to obtain spectra with $\Delta = 72$ ps/channel. These spectra were analysed into four components. Corrections for positron annihilation in the source have been made.

2.3.2. Analysis with the CONTIN (PALS-2) program [7, 12, 13]. In fact, in many cases, e.g. in polymers or porous materials, an assumption of a lifetime distribution due to heterogeneity of the local environment in which positrons annihilate is more realistic. In these cases equation (2) should be replaced by

$$C(t) = \int_0^{\infty} \lambda \alpha(\lambda) \exp(-\lambda t) d\lambda \quad (3)$$

where $\alpha(\lambda)$ is the annihilation rate probability density function (PDF). The fraction of positrons annihilating with rates between λ and $\lambda + d\lambda$ is given by $\alpha(\lambda) d\lambda$ with

$$\int_0^{\infty} \alpha(\lambda) d\lambda = 1. \quad (4)$$

The necessary transformations for converting the positron annihilation rate PDF to the corresponding lifetime, radius, and free-volume PDFs are given in [7].

The computer program CONTIN, originally developed by Provencher [12] and then modified by Gregory and Zhu [13, 14, 7] to CONTIN (PALS-2), is widely used for the analysis of positron lifetime spectra of heterogeneous materials. In CONTIN (PALS-2) the PDF is obtained by using a reference spectrum of the specimen with a single well defined positron lifetime. In the present study, the lifetime spectrum of a well annealed and chemically polished Cu sample with $\tau = 121$ ps was used as a reference spectrum. The total counts of both the sample and reference spectra were about nine millions each.

We installed CONTIN (PALS-2) on our IBM 486DX PC using F77 Fortran 77, version 5.20 under DOS 6.2.

2.4. Doppler broadening of the annihilation γ -line

The 511 keV annihilation γ -line was measured using a high-purity germanium detector of energy resolution 1.17 keV at the 514 keV γ -line of ^{85}Sr . Each spectrum, containing more than 10^6 counts, was collected for 10^4 s. Eight spectra were recorded for each pair of samples.

The annihilation γ -line was characterized with usual shape S - and W -parameters. The S -parameter is defined as the ratio of the number of counts in the annihilation line central region ($0 < |\Delta E| < 0.933$ keV) and the total number of counts N_{tot} in the line. The W -parameter is the ratio of the number of counts in the annihilation line (2.33 keV $< |\Delta E| < 7.31$ keV) wings and N_{tot} .

Liszkay *et al* [15] suggested a method for data analysis which directly shows that the same vacancy defect can be present in a set of samples by checking the linearity of the S -parameter versus the W -parameter curve. Obviously, the method remains valid not only when positrons annihilate from the bulk state and only one defect state, but also when the annihilation takes place in two distinct types of defect. Furthermore, it is easy to prove that the linear interdependence of the S - and W -parameters is valid also in the case of three distinct positron states, provided that the relative intensities of two of them remain constant. In fact, the average value of the S - (W -) parameter for a sample in which three definite states with relative intensities $f_1, f_2, f_3 = 1 - f_1 - f_2$ and $f_1 = af_2$ (where a is a constant) exist, can be written as

$$\begin{aligned} S &= af_2S_1 + f_2S_2 + (1 - af_2 - f_2)S_3 \\ W &= af_2W_1 + f_2W_2 + (1 - af_2 - f_2)W_3 \end{aligned}$$

where $S_1(W_1), S_2(W_2), S_3(W_3)$ are characteristic for the respective states. By eliminating the fraction f_2 , a linear interdependence of S and W can be obtained. In the presence of four states, the linear dependence is possible if the condition $f_1:f_2:f_3 = a:b:c$ (a, b , and c are constants) is valid.

Let us use the term 'defect structure' to briefly designate the presence of a combination of several positron states in a sample, between the relative concentrations of which exist the above-mentioned ratios. Then one can generally say that the linear interrelationship between S - and W -parameters exists for samples with the same defect structure.

3. Results and discussion

3.1. Results obtained with the POSITRONFIT EXTENDED program

The best fit was obtained for four-component analysis of the PAL spectra. The results are shown in table 2.

Taking into account that xerogel is composed of oxide regions and pores located between them, the first component $\tau_1 \approx 175\text{--}215$ ps is attributed mainly to p-Ps (singlet Ps) and free-positron annihilation in oxide regions. This assertion is consistent with fact that τ_1 has its minimum value for sample 4, which contains a small amount of TiO_2 crystalline phase. We consider that the second component $\tau_2 \sim 430\text{--}450$ ps is due to positron annihilation in vacancy-type defects in the homogeneous oxide regions of the samples. The last two

components $\tau_3 \approx 1500\text{--}2000$ ps and $\tau_4 \approx 3700\text{--}7500$ ps are, as is commonly accepted, due to o-Ps annihilation in pores with two different average sizes.

Table 2. The positron lifetimes and intensities obtained with the POSITRONFIT EXTENDED program.

Sample	τ_1 (ps)	I_1 (%)	τ_2 (ps)	I_2 (%)	τ_3 (ps)	I_3 (%)	τ_4 (ps)	I_4 (%)	$I_3 + I_4$
1	198(4)	19.5(8)	439(3)	70.3(7)	2031(80)	8.2(6)	3708(329)	2.0(7)	10.2
2	215(5)	29.9(2)	457(6)	61.8(1)	1695(85)	4.9(2)	6605(195)	3.3(1)	8.2
3	180(3)	26.4(9)	441(4)	67.0(7)	1469(83)	3.7(2)	7579(205)	2.8(1)	6.5
4	174(3)	23.5(7)	431(3)	67.8(6)	1547(44)	6.2(2)	6267(166)	2.50(8)	8.74
5	195(4)	24.7(9)	433(3)	71.2(8)	1649(81)	2.8(1)	6853(308)	1.27(6)	4.07

The last column of table 2, which refers to the probability of o-Ps formation, assumed to be proportional to the concentration of pores, presents the lowest value for sample 5 and the largest for sample 1.

The influence of the heat-treatment temperature can be studied by the comparison of $\tau_3(I_3)$ and $\tau_4(I_4)$ for samples 3 and 4. A decrease in the longest lifetime is observed and the concentration of the small pores is seen to increase whereas that of the larger ones is seen to decrease slightly from the 120 °C to 850 °C heat-treated samples.

The presence of chemically absorbed water in sample 3 was established by the measurements of the infrared absorption, and is in accordance with the results in [3]. Chuang and Tao have shown in [6] that the lifetime of o-Ps located in pores of silica gel increases until the pore surface is entirely covered by water. After that a decrease of o-Ps lifetime was observed due to the reduction of pore sizes by the further absorption of water. As we have no samples with absolutely the same sizes of pores, containing and not containing water, from our results it is not possible to reach any conclusions about the influence of OH radicals on the pick-off o-Ps annihilation.

Results for samples 2 and 3, prepared with $R_{wa} = 4$ and 40 respectively, show that for the larger R_{wa} there is a decrease in the smaller-pore concentration while the longest positron lifetime increases. The results for samples 1 and 2, prepared with different ethanol/alkoxides ratios, show for the smaller pores an increase of the concentration ($\approx 50\%$) and of the lifetime, whereas for the larger pores the concentration is practically unchanged but a decrease of the positron lifetime occurs with increase of R_{ea} .

3.2. Results from data processing with CONTIN (PALS-2)

These results are consistent with those obtained using the POSITRONFIT EXTENDED program. Figure 1 shows as an example the positron annihilation lifetime probability distribution functions for samples 3 and 4 obtained using the CONTIN (PALS-2) program.

It should be noted that although the shortest lifetime distribution is not very reliable because of the lifetime resolution of ~ 260 ps of the spectrometer, the resolution has only a minor influence on the longer distributions of τ_3 and τ_4 , which are the lifetimes of interest in the present study [6, 7]. The results for the two longest lifetimes τ_3 and τ_4 , as well as their relative intensities, obtained using CONTIN (PALS-2) are shown in table 3. The last column in the table contains the experimental fraction, $\Phi_2(\beta) = I_3/(I_3 + I_4)$, of o-Ps annihilated in oxide particles (see the text below).

A semiempirical equation relating the measured o-Ps lifetime and the free-volume hole

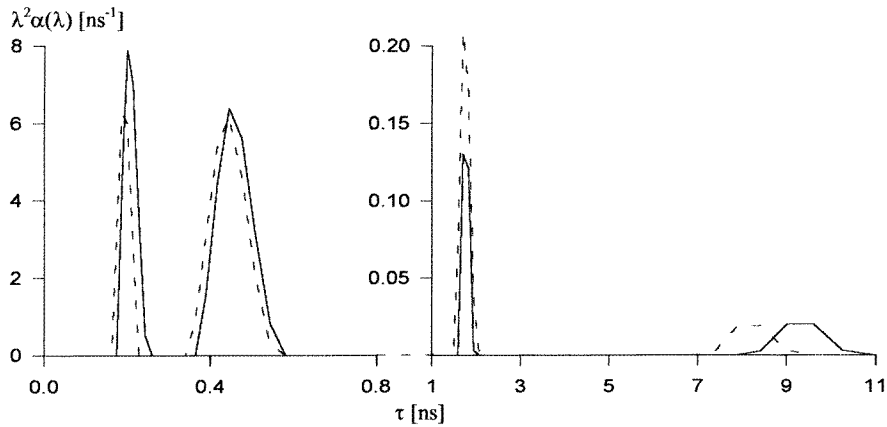


Figure 1. The positron annihilation lifetime PDFs for samples 3 (—) and 4 (---).

Table 3. The o-Ps average lifetime parameters obtained using CONTIN (PALS-2).

Sample	τ_3 (ns)	Positron fraction	τ_4 (ns)	Positron fraction	$\Phi_2(\beta)$
1	2.25	0.093	5.78	0.007	0.93
2	2.00	0.044	8.28	0.030	0.59
3	1.73	0.028	9.37	0.027	0.51
4	1.73	0.057	8.23	0.023	0.71
5	1.99	0.022	10.05	0.012	0.65

radius R has been obtained [16, 17]:

$$\tau = \frac{1}{2} [1 - R/(R + R_w) + (1/2\pi) \sin(2\pi R/(R + R_w))]^{-1} \quad (5)$$

where τ and R are expressed in ns and \AA , respectively and R_w takes the value 1.656 \AA .

Using the corresponding transformation formulae from [7] and equation (5), the radius PDFs were obtained from the Ps lifetime probability distribution functions. The fraction of positrons annihilating in cavities with radii between R and $R + dR$ is $f(R) dR$, where $f(R)$ is the radius PDF and is given by

$$f(R) = |2R_w \{ \cos 2\pi R/(R + R_w) - 1 \} \alpha(\lambda) / (R + R_w)|. \quad (6)$$

The free-volume PDF assuming a spherical cavity is $g(V) = f(R)/4\pi R^2$. The fraction of positrons annihilating in cavities with volumes between V and $V + dV$ is $g(V) dV$.

The radius PDFs are presented on figure 2 in such a way that the influence of R_{wa} and R_{ea} , as well as of the heat treatment, on the pore sizes can be seen.

PAL measurements reveal the existence of pores with two different sizes provided that the same annihilation rate/pore radius correlation (5) is valid for both species—the small pores with average diameter $\leq 6 \text{ \AA}$ and larger pores with average diameters ranging from 10 to 13 \AA .

For the 10 mol% TiO_2 composition heat treated at $120 \text{ }^\circ\text{C}$, the sample prepared with the larger R_{ea} -ratio (sample 1) shows the largest small pores with the greatest concentration, and the smallest large pores with the lowest concentration. The defect structure of sample 3, prepared with larger water content, is just the opposite. Sample 3 shows smaller small pores with low concentration, and larger large ones with comparatively high concentration.

These results indicate that the oxide network of xerogel treated at 120 °C is very open. In the case of sample 1 there is essentially a one-size pore distribution of small pores with large concentration, whereas the sample prepared with larger water content, sample 3, shows a larger concentration of pores with two pore size distributions. When such a sample is heat treated at 850 °C it becomes sample 4. PAS results for this sample show that the essential difference introduced by heat treatment at such a temperature is the decrease in both size and concentration of the large pores.

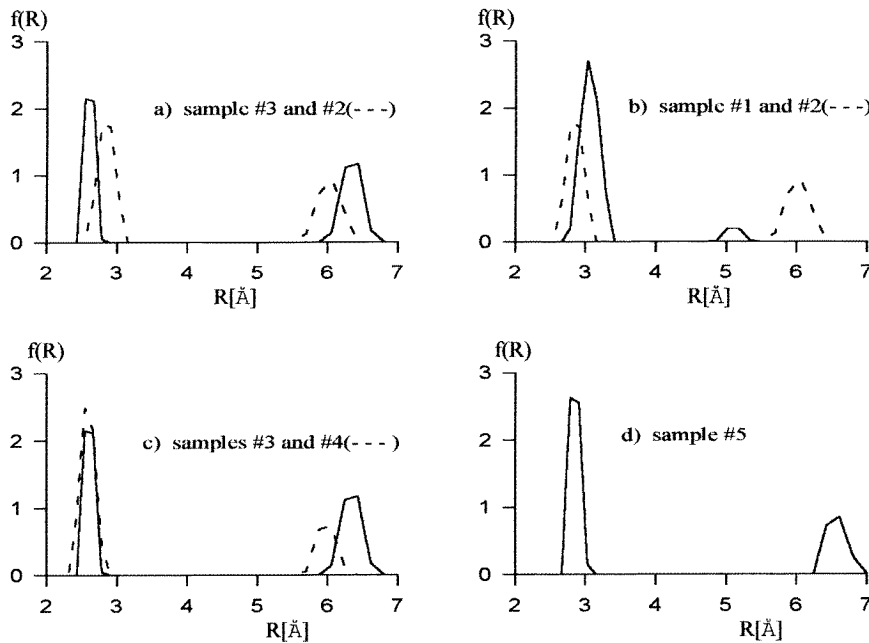


Figure 2. Radius PDFs.

The higher-TiO₂-content sample presents a PDF similar to those of the other samples. As the influence of the water on o-Ps lifetimes is not clear, all of the following numerical evaluations refer to sample 4.

The presence of pores with two different average sizes in $x\text{TiO}_2 \cdot (1-x)\text{SiO}_2$ as well as the results of SANS studies [3] of xerogels are compatible with the assumption that the physical structure of dried silica-titania gels is similar to that of dried silica gel [6]. It is composed of closely bounded homogeneous oxide regions (particles) with finer pores located within these regions and larger ones between them. There is a certain probability for the o-Ps, formed in such a sample, to diffuse into the larger pores, be trapped there, and survive inside them over the course of a mean time τ_4 (from 6 to 10 ns). The third component with a mean lifetime $\tau_3 \sim 1.7\text{--}2.2$ ns can be attributed to the pick-off annihilation of o-Ps before it diffuses into the larger pores. Following the method proposed by Chuang and Tao [6] it is possible to evaluate the diffusion constant, D , of o-Ps in silica-titania gel, assuming that the oxide particles are spherical in shape and that the connecting bridges between them are thin. Under these assumptions the fraction, $\Phi_2(\beta)$, of all o-Ps atoms annihilating inside oxide particles with mean radius r , can be calculated from the formula

$$\Phi_2(\beta) = 1 - 1.5\beta[1 - \beta^2 + (1 + \beta)^2 \exp(-2/\beta)] \quad (7)$$

where $\beta = (D\tau_3)^{1/2}/r$.

Inserting in (7) our experimental values of $\Phi_2(\beta) = 0.71$ and $\tau_3 = 1.73$ ns for sample 4, which does not contain water, the value $D = 0.58 \times 10^{-5}$ cm² s⁻¹ has been derived provided that the mean particle radius for $x = 10$ mol% TiO₂ is the same as was obtained for $x = 2, 4$ and 6 mol% (about 5 nm) [3]. This value of D is one order of magnitude smaller than D for silica gel [6] with $r \approx 2$ –3 nm.

It is interesting to note that if the structure of dried silica–titania gel is composed of closely packed spherical oxide particles with radius r , from purely geometrical considerations the radius R of the inscribed pores is $R = 0.23r$. From the experimentally obtained value $R = 0.6$ nm (sample 4), the mean radius of the oxide particles is evaluated to be $r = 2.6$ nm, i.e. of the same order of magnitude as that used above.

3.3. Doppler broadening of annihilation lines

The S -parameter as a function of the W -parameter is presented in figure 3. As can be seen, only the points corresponding to samples 1, 2 and 3 lie on the same straight line. Hence, only these samples have the same defect structure (see section 2.4), although prepared with different water/alkoxides and ethanol/alkoxides molar ratios. The experimental point for sample 5 lies near the straight line, whereas that for sample 4 is far away, as if the heat treatment had greater influence on the defect structure than the TiO₂ content.

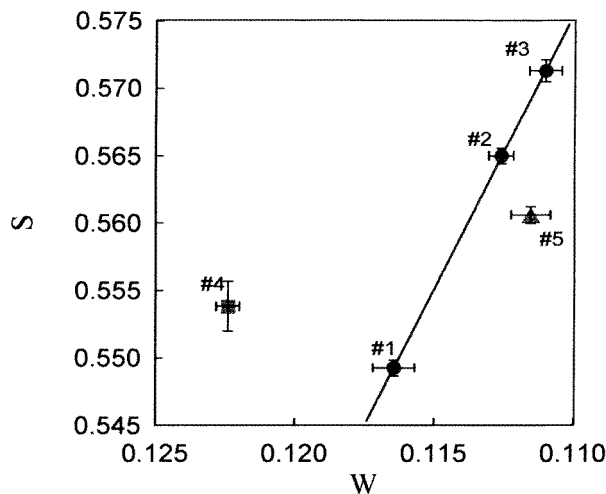


Figure 3. The S -parameter as a function of the W -parameter.

Acknowledgments

This work was partially supported by the International Atomic Energy Agency under Contracts No 7567/RB and No 7284/RB and by JNICT contract No PBIC/C/CIM/1396/92.

We thank Dr Provencher for sending us a User's Manual and Professor Gregory for sending us the CONTIN (PALS-2) computer code.

References

- [1] Yang L and You G 1988 *J. Non. Cryst. Solids* **100** 309
- [2] Salvado I M M and Navarro J M F 1990 *J. Matter Sci. Lett.* **9** 173; 1992 *J. Non-Cryst. Solids* **147+148** 256
- [3] Margaca F 1994 *Report of the First RCM of the Co-ordinated Research Programme on 'Advanced Ceramic Materials Characterization using Thermal Neutrons'* IAEA, Vienna
- [4] Ramani R, Ramachandra P, Ravichandran T S G, Ramagopal G, Gopal S and Ranganathaiah C 1995 *Appl. Phys. A* **60** 481
- [5] Leidheiser H Jr, Szeles C and Vertes A 1987 *Nucl. Instrum. Methods A* **255** 606
- [6] Chuang S Y and Tao S J 1971 *J. Chem. Phys.* **54** 4902
- [7] Gregory R 1991 *J. Appl. Phys.* **70** 4665
- [8] Dai G H, Deng Q, Liu J, Shi H, Huang C M and Jean Y C 1993 *J. Physique. IV Coll. Suppl.* **3** C4 233
- [9] Wang C L and Wang S J 1995 *Phys. Rev. B* **51** 8810
- [10] Jean Y C 1990 *J. Microchem.* **42** 72
- [11] Kirkegaard P, Eldrup M, Mogensen O E and Pedersen N J 1981 *Comput. Phys. Commun.* **23** 307
- [12] Provencher S W 1982 *Comput. Phys. Commun.* **27** 229
- [13] Gregory R B 1990 *Positron and Positronium Chemistry* ed Y C Jean (Singapore: World Scientific) p 136
- [14] Gregory R B and Zhu Y 1990 *Nucl. Instrum. Methods Phys. Res. A* **290** 172
- [15] Liskay L, Corbel C, Baroux L, Hautojärvi P, Bayhan M, Brinkman A W and Tatarenko S 1994 *Appl. Phys. Lett.* **64** 1380
- [16] Nakanishi H, Wang S J, and Jean Y C 1988 *Positron Annihilation Studies of Fluids* ed S C Sharma (Singapore: World Scientific) p 292
- [17] Jean Y C 1995 *Mater. Sci. Forum* **175-178** 59